Development and Validation of a 95th Percentile Male Pedestrian Finite Element Model

Wansoo Pak[1], Costin D. Untaroiu[1]

[1]*Virginia Tech, Blacksburg, VA, USA*

Abstract

The pedestrian is one of the most vulnerable road users. Given an impact event, the probability of a pedestrian fatality in a traffic crash is almost two times higher than that for a vehicle occupant. Therefore, pedestrian protection regulations which involve subsystem tests in car-to-pedestrian collisions (CPC) have been proposed in Europe and Asia. In addition, human finite element (FE) models have been developed to better understand the whole vehicle-pedestrian interaction, and assess the pedestrian injuries. However, the majority of these human models represent a 50th percentile human, so their responses cannot be extrapolated to understand the responses of pedestrian with other anthropometries during a CPC. The main goal of this study was to develop and validate a FE model corresponding to a 95th percentile male (M95) pedestrian. The model mesh was developed by morphing the Global Human Body Models Consortium (GHBMC) 50th percentile male (M50) pedestrian model to the reconstructed geometry of a human subject having 194 cm height and 103 kg weight. The material properties of the M95 pedestrian model were assigned based on GHBMC M50 occupant model. The knee joint and upper torso of the FE model were preliminarily validated against Post Mortem Human Surrogate (PMHS) test data recorded in four-point knee bending tests and upper body blunt lateral impact tests. Then, pedestrian-to-vehicle impact simulations were performed using the whole pedestrian model and the results were compared to corresponding pedestrian PMHS tests. Overall, the results generated by the FE model showed to be well correlated to test data. Therefore, the model could be used to investigate various pedestrian accidents or to improve vehicle front end design for pedestrian protection.

Introduction

Pedestrians represent one of the most vulnerable road users. Every year, more than 270,000 pedestrian fatalities were recorded in the world which comprise of 22% of all road traffic fatalities [1]. In the United States, 4,735 pedestrians were killed and approximately 66,000 injured in road crashes in 2013 [2]. Therefore, protection of pedestrians in the CPC has recently generated increased attention with regulations which involve three subsystem tests for adult pedestrian protection (leg, thigh and head impact tests). While these subsystem tests can help in reducing the stiffness of vehicle front end components and consequently reduce the risk of injuries, neither the complex pedestrian-vehicle interaction nor the injury mechanisms can be characterized by these simple impact tests. Therefore, several human FE models of pedestrians have been developed and pedestrian accidents have started to be investigated numerically.

High biofidelity computational human models could predict both pedestrian kinematics and risks of injuries during a CPC, and therefore could be useful in the development of new pedestrian-friendly vehicles. Several pedestrian FE models representing 50th percentile males have been developed and validated previously [3, 4] . However, the pedestrian anthropometry

plays a major role in pedestrian kinematics and injury mechanisms during a CPC [5-7], so new FE models with various anthropometries are needed to be developed to cover the whole human variation. The primary goal of this study was to develop and validate a FE model corresponding to a 95th percentile male anthropometry in standing posture.

Methods

The M95 pedestrian FE model was developed from a subject (194 cm and 103 kg) who was recruited to match target anthropometry for 95th percentile male body size. The mesh of the model was obtained by morphing a linear scaled version of the M50 model to the final target geometry using a radial basis interpolation approach [8]. The defined material properties of the model were based on the GHBMC 50th percentile male occupant model. First, the pedestrian FE model was validated at component level under impact loadings applied to the knee joint and the upper torso. Then, the whole body model was validated in a CPC scenario. The whole validation process is presented in the following sections.

Validation of the knee joint under valgus bending

Valgus bending and shearing of the knee joint have been recognized as primary injury mechanisms during a CPC accident [9]. To validate the biomechanical and injury response of the knee joint under lateral loading, a four-point bending PMHS test reported in the literature was simulated [9]. The tested knee joints were acquired from 24 adult PMHS (68.3 ± 9.8 ages, 172 ± 7.8 cm height and 75.2 ± 14.4 kg weight). The knee joint FE model was extracted from the GHBMC 95th percentile male pedestrian FE model and then re-positioned to fit into the simulation setup (Figure 1). The ends of the three bones (femur, fibula and tibia) were assigned as rigid (*MAT_020 [10]) and constrained to the bone cups. All test setup parts were defined as rigid except the load cell attached to the bone cup, which was assigned as deformable material in order to calculate the bending moment using a cross-section card [10]. The bone cups were attached to extension bars that were linked to the rotational joint supports. The support on the femur side was allowed to slide horizontally, while the other support was fixed. To load the knee joint under valgus bending, the extension bars were rotated at a knee angular rate of approximately 1 deg/ms in correspondence with a 40 km/h CPC [11]. In the simulation, the time histories of angular velocities were imposed to the rigid bars based on the data recorded in the PMHS tests.

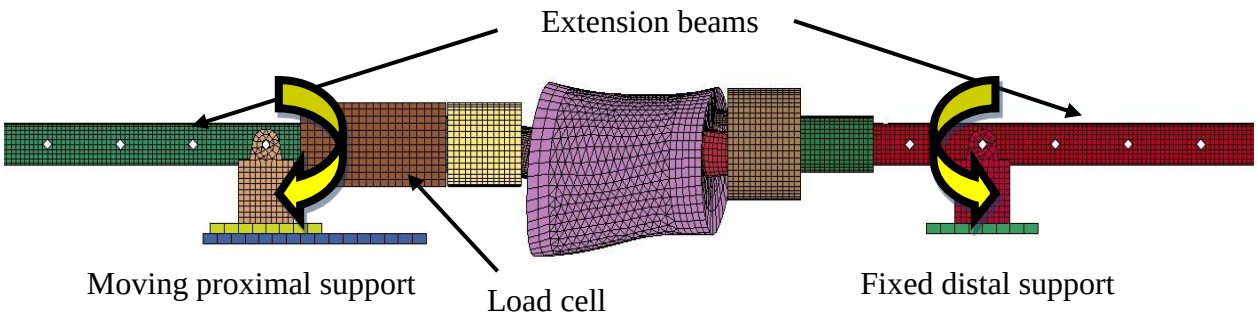

Figure 1. The schematic FE simulation setup of four-point knee joint bending

Validation of the upper torso

The upper torso section of the whole body FE model was validated against test data recorded on 14 PMHS specimens (53.8 ± 13.9 age, 67.2 ± 16.2 kg weight) in blunt lateral impact loading [12]. The specimen was suspended upright with arms overhead then released at impact. A 23.4 kg rigid impactor was freely suspended by a guided string and accelerated approximately to 4.5, 6.7 or 9.4 m/s pre-impact speeds.

Based on the *in-vitro* test data, eight FE simulations were performed using the pedestrian model with different combinations of impacted regions (pelvis, abdomen and thorax) and impactor initial speeds. To avoid interference between arm and impactor during validation, the arm parts were removed but the mass of arm was applied near each scapular region to maintain the same pedestrian total mass (Figure 2). The pelvis was loaded laterally (Figure 2 a) with the impactor aligned adjacent to the greater trochanter. The center of the impactor was aligned to the xiphoid process for the thorax impact and 7.5 cm down from the xiphoid process for the abdomen impact. Then, the impactor was rotated 60° from the anterior-posterior direction of the model before to impact the model (Figure 2 b, c).

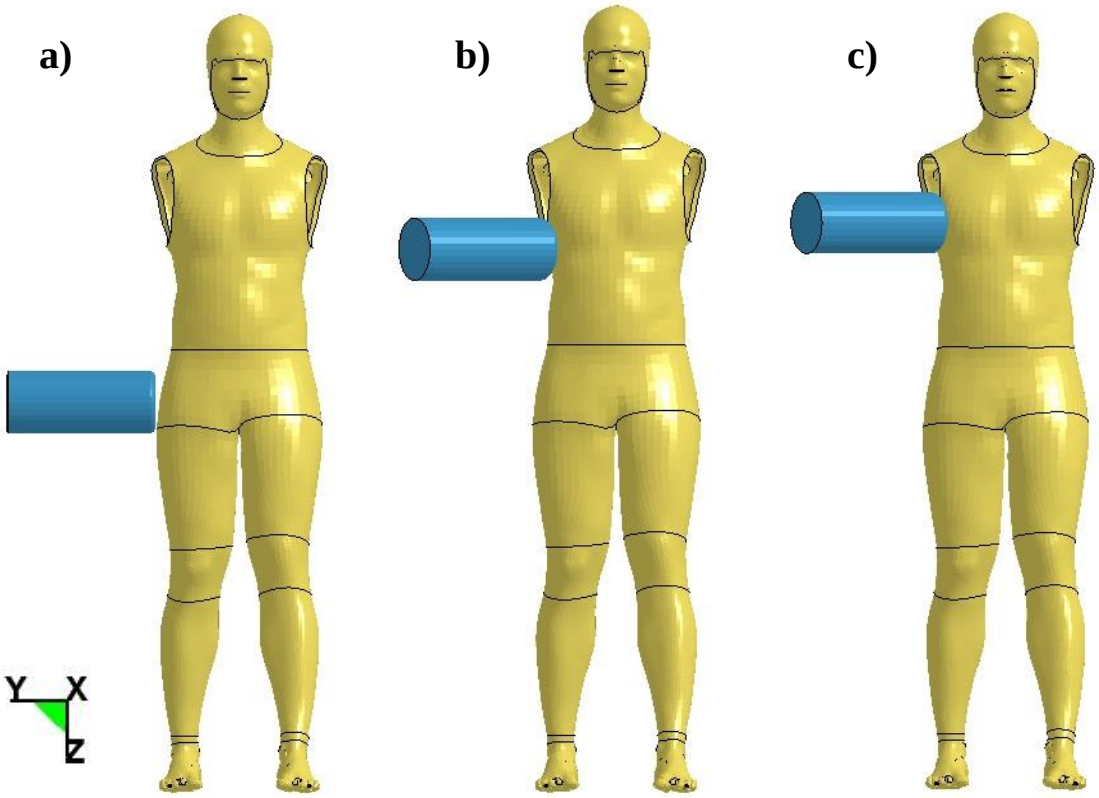

Figure 2. The lateral impact FE simulation setup: **a)** Pelvis **b)** Abdomen **c)** Thorax

Validation of the whole body

The whole body FE model of 95th pedestrian male was validated in a CPC simulation against PMHS pedestrian data [13]. The pedestrian model was positioned laterally in a mid-stance posture at the centreline of a mid-sized sedan FE model (Figure 3). In testing, the PMHS

was supported by a harness and released approximately 20-30 ms before the vehicle contact. In FE simulation, prior the impact (5 ms), the gravity acceleration was assigned to the pedestrian model and a force corresponding to its weight was applied upward by the ground model (Figure 3). Then, the vehicle with 40 km/h initial velocity impacted the pedestrian FE model. As in testing, the kinematic trajectories of head's centre of gravity (CG), first thoracic vertebra (T1) and sacrum relative to the car were recorded during the car impact and compared against the PMHS test data [13].

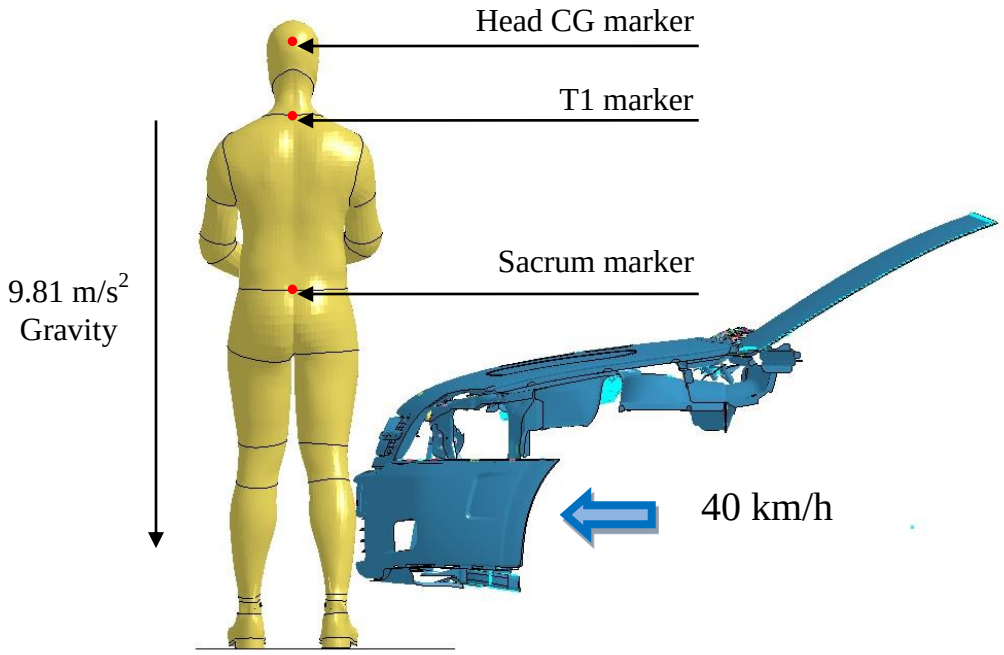

Figure 3. The FE simulation setup of the car-to-pedestrian whole body validation

Results and Discussion

The results of each FE simulation at the component level were calculated and then filtered (SAE 180) before being compared against corresponding PMHS test data. Then, the unfiltered kinematic trajectories of the whole body validation were compared against corresponding test data. Due to the lack of PMHS data for M95 subjects, the impact responses of the pedestrian model were compared to existing test corridors scaled to M50 anthropometry.

Validation of M95 Pedestrian Model at component level

Overall, the curve of angular bending stiffness corresponding to M95 FE model has a similar shape as the curve corresponding to M50 FE model [14] (Figure 4). However, higher stiffness than the curves corresponding to M50 and scaled PMHS data can be observed in the M95's response possibly due to its higher stature. During the first phase of loading, lower values of the load cell bending moments of both M95 and M50 are observed in the simulations compared to testing. This discrepancy is likely caused by the setup inertia which was approximated in the FE model. As in the M50 knee model, the M95 knee model predicted MCL and ACL injuries in a range from 14^0 up to 17.5^0 knee angles. It should be mentioned that these

ligament injuries were the most frequent injuries observed, with52.5% (MCL) and 10 % (ACL) injuries being observed in all PMHS knee bending tests [9].

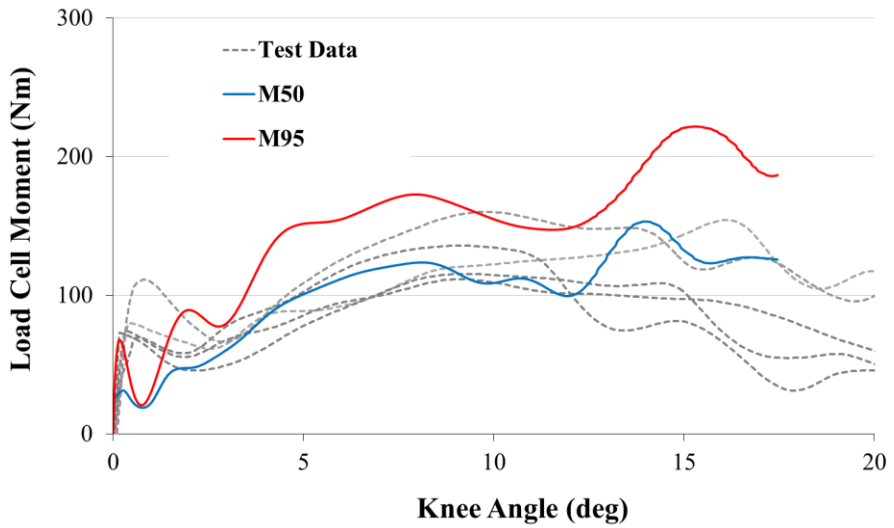

Figure 4. The result of knee bending: FE simulation vs. PMHS tests

The impact force time histories predicted by the M95 FE model under pelvic lateral loading were close the mean corridor at lower impact velocity (5.2 m/s) and close to the upper boundary corridor at higher impact velocity (9.8 m/s) (Figure 5). Since the pelvic flesh plays a significant role in this impact test, it is believed that a more biofidelic material model of flesh may improve the response of the model in this loading condition. Therefore, it is recommended updating the material model of flesh when compression test data on pelvic flesh specimens becomes available.

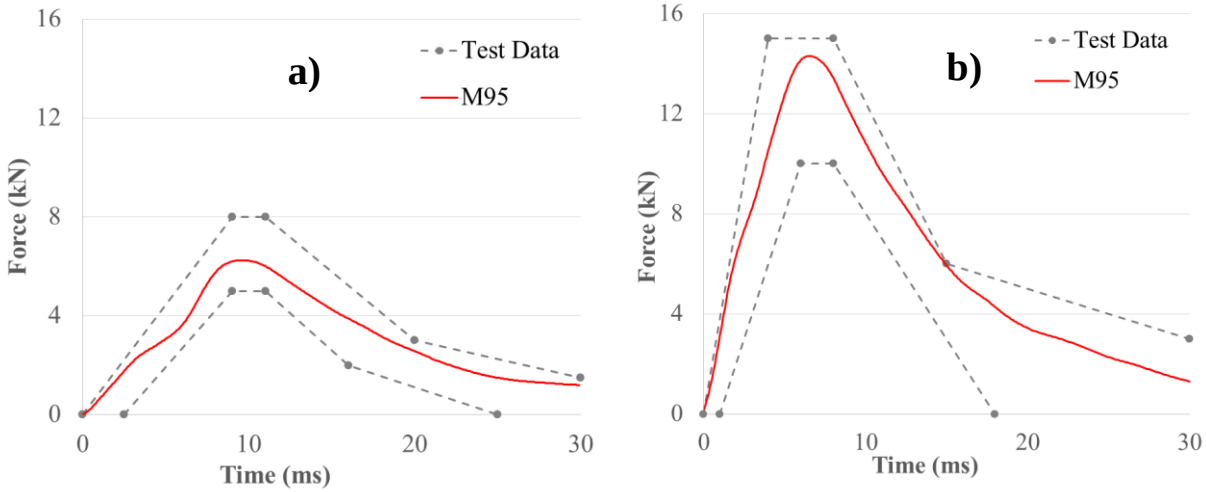

Figure 5. Pelvis impact. The time histories of impact force: FE model vs. PMHS test data a) 5.2 m/s impactor initial velocity, b) 9.8 m/s impactor initial velocity

The time histories of impact force predicted by the M95 upper torso model were compared against the PMHS test data recorded at thorax location (Figure 6) and abdomen

location (Figure 7) and then normalized to M50 [12]. At the beginning of the FE simulations (approximately 0 to 5 ms), the impact force gradients were close to the upper corridor of the PMHS test data. These results were expected due to the higher mass of M95 than that of M50. However, after the first peak force, a larger decrease of the impact force predicted by the M95 model than the normalized PMHS corridor is observed. While the internal organs were not modeled and included in the current version of M95, the rib cage is the main contributor to its stiffness. Therefore, it is believed that modeling internal organs [15] and including them into the rib cage cavity will improve the damping properties of the torso and consequently the overall correlation of the model with the PMHS test data.

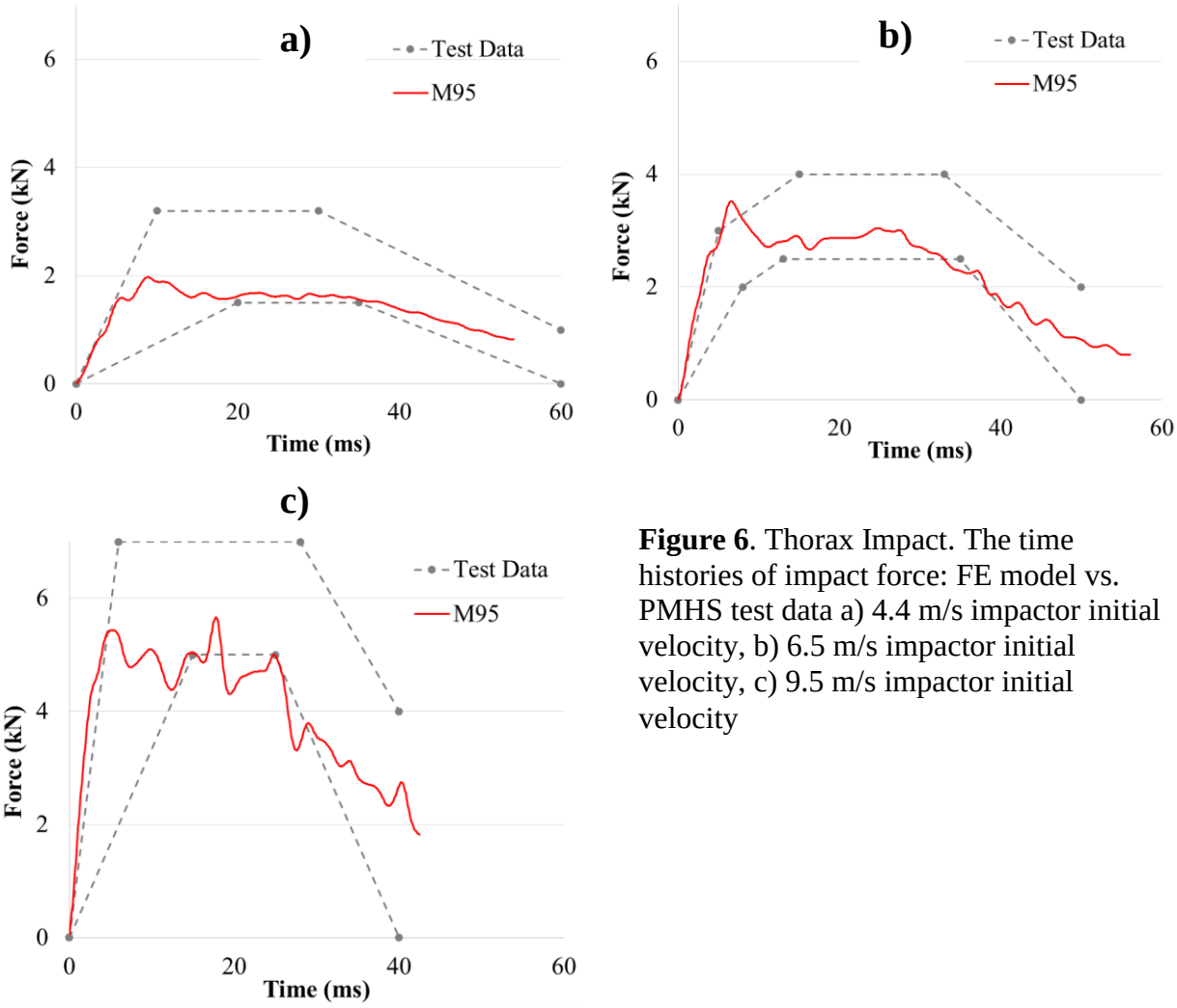

Figure 6. Thorax Impact. The time histories of impact force: FE model vs. PMHS test data a) 4.4 m/s impactor initial velocity, b) 6.5 m/s impactor initial velocity, c) 9.5 m/s impactor initial velocity

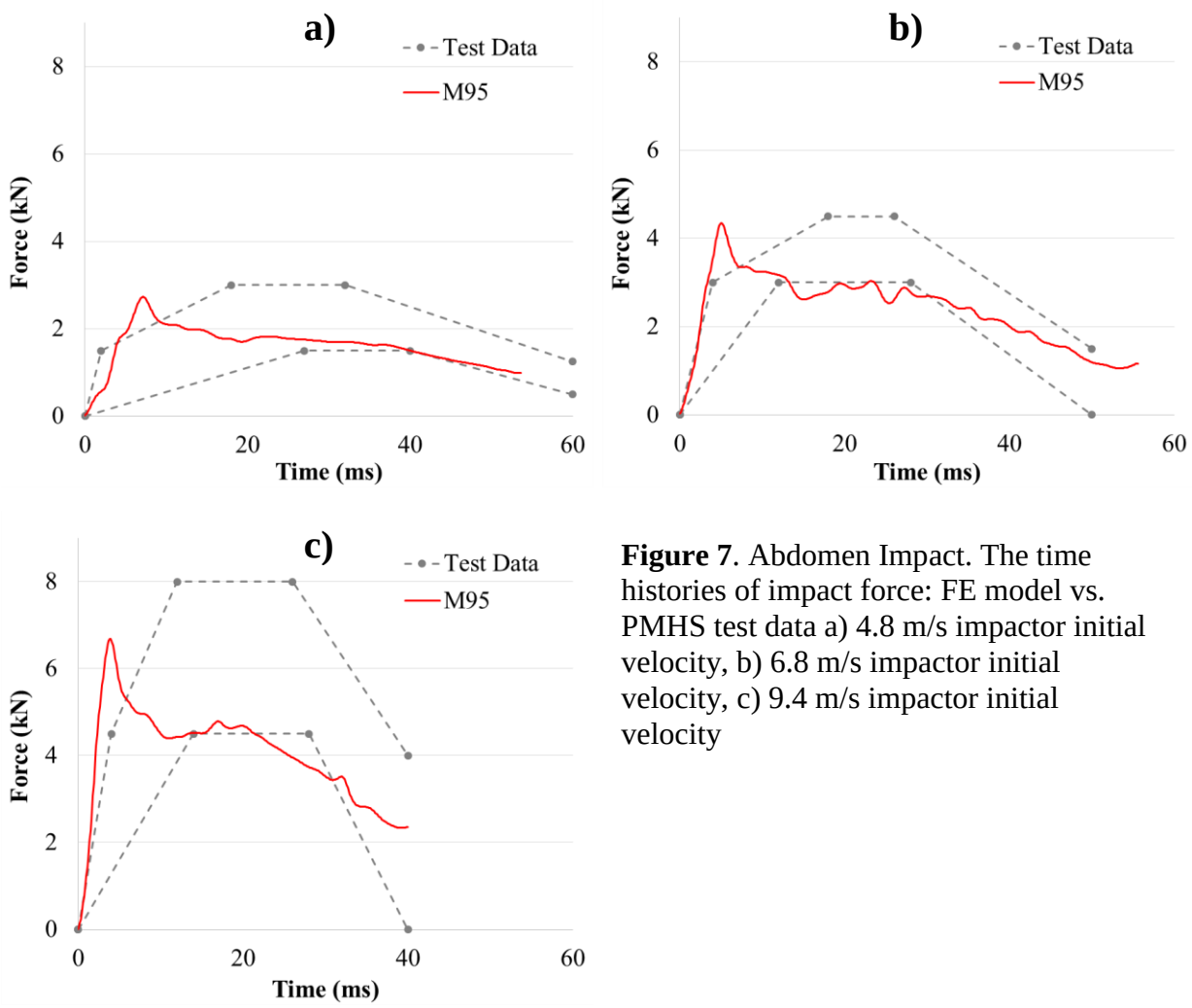

Figure 7. Abdomen Impact. The time histories of impact force: FE model vs. PMHS test data a) 4.8 m/s impactor initial velocity, b) 6.8 m/s impactor initial velocity, c) 9.4 m/s impactor initial velocity

Validation of M95 Pedestrian Model in CPC simulation

The overall trajectory of M95 upper body model showed to be close to the trajectories recorded on tall PMHS test data (Figure 8). As it can be observed, the Head CG and T1 trajectories predicted by the pedestrian FE model were similar at the beginning and slightly above to the corresponding trajectories recorded on tall PMHS subjects. This could be caused by higher stature of the FE model compared to the tall PMHS (194 cm of FE model vs. 179 and 184.3 cm of PMHSs). In terms of injuries, the M95 model predicted knee injuries in both right (the first leg impacted) and left lower extremities. While ligament injuries of right knee were recorded in one PMHS, bone fractures (mostly tibia fractures) were the most common injury pattern in PMHS right lower extremities (six of seven tests). The initial position of the bumper relative to the M95 right knee is different than in PMHS due to the higher stature of M95. This generates a different loading pattern and consequently be the cause of different injuries predicted by M95 right lower limb. In the left lower extremity, the typical injury pattern in PMHS tests was LCL/ACL rupture (5 tests) as the injuries predicted by the pedestrian M95 model. To better understand the overall contributions of pedestrian anthropometry and lower limb material/failure properties a sensitivity study [16-18] is suggested to be performed in the future.

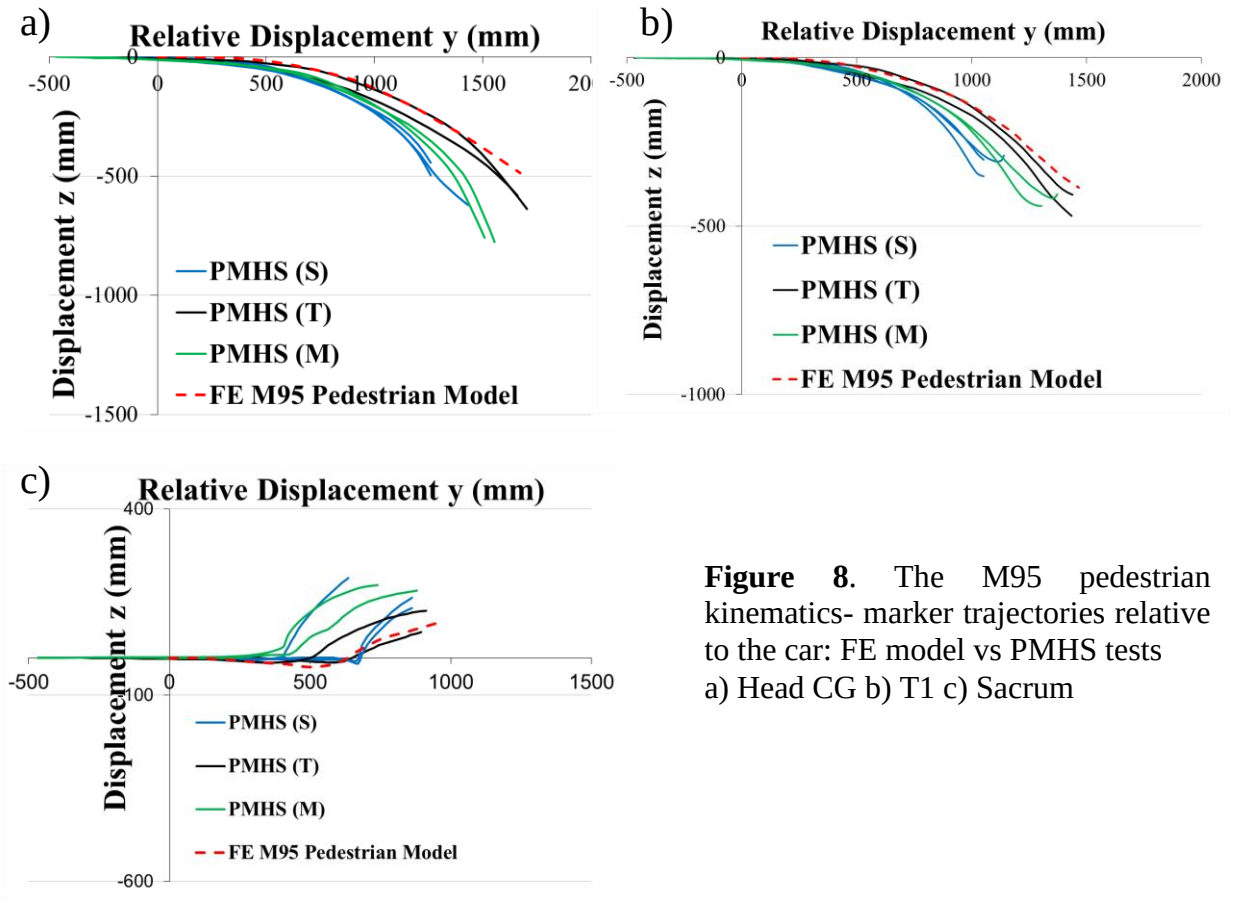

Figure 8. The M95 pedestrian kinematics- marker trajectories relative to the car: FE model vs PMHS tests
a) Head CG b) T1 c) Sacrum

Conclusions

In this study, a 95th percentile male pedestrian FE model was developed and validated against the corresponding PMHS test data. The validation was implemented at component level against knee joint tests under valgus bending and upper torso lateral impacts. Then, the whole body FE model was validated in CPC impact against the PMHS test data. Overall, the model showed promising results and a good capability to predict the injury risk of pedestrian during lateral car impact.

Acknowledgements

Funding for this study was provided by the Global Human Body Models Consortium (GHBMC). All findings and views reported in this manuscript are based on the opinions of the authors and do not necessarily represent the consensus or views of the funding organization. The authors would also like to acknowledge the help received from Dr. Scott Gayzik's team (Wake Forest University) with the initial development of the model by morphing.

References

[1] W. H. Organization, "Global status report on road safety," 2013.
[2] NHTSA, "2013 Data: Pedestrians," 2013.

[3] Y. Takahashi, Y. Kikuchi, A. Konosu, and H. Ishikawa, "Development and validation of the finite element model for the human lower limb of pedestrians," *Stapp car crash journal*, vol. 44, pp. 335-55, 2000.

[4] C. D. Untaroiu, J. B. Putnam, J. Schap, M. L. Davis, and F. S. Gayzik, "Development and preliminary validation of a 50th percentile pedestrian finite element model," in *ASME 2015 IDETC/CIE Conference*, Boston, MA, USA, 2015, p. 7.

[5] R. Fredriksson, J. Shin, and C. D. Untaroiu, "Potential of pedestrian protection systems--a parameter study using finite element models of pedestrian dummy and generic passenger vehicles," *Traffic injury prevention*, vol. 12, pp. 398-411, 2011.

[6] C. D. Untaroiu, J. Shin, J. R. Crandall, R. Fredriksson, O. Bostrom, Y. Takahashi, *et al.*, "Development and validation of pedestrian sedan bucks using finite-element simulations: a numerical investigation of the influence of vehicle automatic braking on the kinematics of the pedestrian involved in vehicle collisions," *International Journal of Crashworthiness*, vol. 15, pp. 491-503, 2010.

[7] R. Watanabe, T. Katsuhara, H. Miyazaki, Y. Kitagawa, and T. Yasuki, "Research of the relationship of pedestrian injury to collision speed, car-type, impact location and pedestrian sizes using human FE model (THUMS Version 4)," *Stapp car crash journal*, vol. 56, pp. 269-321, 2012.

[8] N. A. Vavalle, S. L. Schoell, A. A. Weaver, J. D. Stitzel, and F. S. Gayzik, "Application of radial basis function methods in the development of a 95th percentile male seated fea model," *Stapp car crash journal*, vol. 58, p. 361, 2014.

[9] D. Bose, K. S. Bhalla, C. D. Untaroiu, B. J. Ivarsson, J. R. Crandall, and S. Hurwitz, "Injury tolerance and moment response of the knee joint to combined valgus bending and shear loading," *J Biomech Eng*, vol. 130, p. 031008, Jun 2008.

[10] LSTC, "LS-DYNA KEYWORD USER'S MANUAL," ed, 2013.

[11] C. Untaroiu, K. Darvish, J. Crandall, B. Deng, and W. Jenne-Tai, "A finite element model of the lower limb for simulating pedestrian impacts," *Stapp car crash journal*, vol. 49, p. 157, 2005.

[12] D. C. Viano, "Biomechanical responses and injuries in blunt lateral impact," SAE Technical Paper 0148-7191, 1989.

[13] J. R. Kerrigan, J. R. Crandall, and B. Deng, "Pedestrian kinematic response to mid-sized vehicle impact," *International journal of vehicle safety*, vol. 2, pp. 221-240, 2007.

[14] C. D. Untaroiu, J. B. Putnam, J. Schap, M. L. Davis, and F. S. Gayzik, "Development and Preliminary Validation of a 50th Percentile Pedestrian Finite Element Model," in *ASME 2015 International Design Engineering Technical Conferences and Computers and Information in Engineering Conference*, 2015, pp. V003T01A004-V003T01A004.

[15] Y. C. Lu and C. D. Untaroiu, "A statistical geometrical description of the human liver for probabilistic occupant models," *Journal of Biomechanics*, vol. 47, pp. 3681-3688, Nov 28 2014.

[16] J. B. Putnam, J. T. Somers, and C. D. Untaroiu, "Development, calibration, and validation of a head-neck complex of THOR mod kit finite element model," *Traffic injury prevention*, vol. 15, pp. 844-54, 2014.

[17] Y. Han, J. K. Yang, K. Mizuno, and Y. Matsui, "Effects of Vehicle Impact Velocity, Vehicle Front-End Shapes on Pedestrian Injury Risk," *Traffic Injury Prevention*, vol. 13, pp. 507-518, 2012.

[18] L. M. Saez, L. J. G. Casanova, E. A. Fazio, and A. G. Alvarez, "Behaviour of high bumper vehicles in pedestrian scenarios with full finite element human models," *International Journal of Crashworthiness*, vol. 17, pp. 1-10, Feb 2012.